



Straw return strategies for soil microbial quotient enhancement: Insights from DOM vertical distribution characteristics



Yuanchen Zhu^{a,1}, Wei Yang^{a,b,1}, Juanjuan Qu^b, Yue Jiang^b, Ying Zhao^a, Zhimin Wu^a, Jie Su^{a,b}, Xiaozeng Han^a, Wenxiu Zou^{a,*}

^a State Key Laboratory of Black Soils Conservation and Utilization, Northeast Institute of Geography and Agroecology, Chinese Academy of Sciences, Harbin 150081, China

^b School of Resources and Environment, Northeast Agricultural University, Harbin 150030, China

ARTICLE INFO

Keywords:

Straw return
Soil microbial quotient
Dissolved organic matter
Fluorescence spectroscopy
Soil depth

ABSTRACT

The soil microbial quotient (SMQ), a critical indicator of agricultural soil quality, exhibits significant responsiveness to dissolved organic matter (DOM). However, how the heterogeneity of DOM characteristics regulates the SMQ remains unclear, despite DOM being a critical energy source for microorganisms. We conducted a field experiment with four treatments: conventional tillage (CT), no-till with straw mulch (NTS), conventional tillage with straw mulch and incorporation (CTS), and deep tillage with straw incorporation (DTS), with soil samples collected at four depth intervals (0–10, 10–20, 20–30, and 30–40 cm) to investigate how DOM characteristics influence SMQ. The results indicated that SMQ declined with soil depth. Straw return enhanced SMQ, with effectiveness ordered as CTS > NTS > DTS > CT. Compared to CT, straw return increased the content and humic-like components of DOM. Additionally, NTS and CTS accelerated depth-dependent variations in protein-like substances, whereas DTS promoted those in humic-like substances. Linear regression analysis showed that SMQ was positively correlated with both dissolved organic carbon and humic-like components of DOM. Random Forest analysis showed that soil enzyme activities and nutrients dominated SMQ regulation in the 0–20 cm layer, while DOM characteristics governed SMQ in the 20–40 cm layer. Among all treatments, CTS was identified as the most effective in enhancing SMQ. These findings elucidate the DOM-mediated mechanism of SMQ regulation under straw return, providing a scientific basis for optimizing agricultural management practices.

1. Introduction

Although microbial biomass carbon (MBC) constitutes only 1–5 % of soil organic carbon (SOC), it serves as a metabolically active component that plays a vital role in promoting the decomposition of plant residues and the formation of soil organic matter (Sun et al., 2020b; Wang et al., 2024b). Soil microbial quotient (SMQ), defined as the ratio of MBC to SOC, is widely recognized as an early indicator of soil health, with higher values generally reflecting better soil quality (Bhaduri et al., 2022; Ding et al., 2024; Wang et al., 2025). SMQ was observed to exhibit significant variations in the soil profile (Sun et al., 2020b). Soil biotic (e.g., enzyme activity) and abiotic factors (e.g., pH and nutrient availability) collectively control SMQ by influencing soil microbial activity and exogenous carbon transformation (Cong et al., 2020; Chen et al., 2022; Gao et al., 2024). However, studies exploring the vertical

distribution of SMQ and its controlling mechanisms remain scarce, which is critical for understanding soil microbial biogeography.

Dissolved organic matter (DOM), as the most dynamic and reactive component of soil organic matter, can regulate SMQ by influencing soil biogeochemical processes (Ding et al., 2022; Zhang et al., 2024). It has been shown that higher dissolved organic carbon (DOC) content provides a sufficient energy source for microorganisms, thereby potentially enhancing microbial activity (Song et al., 2022a). Several studies have confirmed that higher content of humic-like components in DOM reduces microbial metabolic quotient and thus increases SMQ (Yang et al., 2024c; Tang et al., 2024a). In addition, DOM exhibits pronounced vertical heterogeneity in the soil profile, driven by differences in soil physicochemical properties (e.g., pH) and biogeochemical processes (e.g., microbial DOM fixation, release, and metabolism) across different soil layers (Liu et al., 2023a; Huang et al., 2024; Xiao et al., 2025).

* Corresponding author.

E-mail address: zouwenxiu@iga.ac.cn (W. Zou).

¹ These authors contributed equally to this article and should be considered as co-first authors.

However, how vertical heterogeneity of DOM influences the vertical distribution of SMQ remains poorly understood.

As one of the most important agricultural management practices, straw return can significantly alter the characteristics of DOM (Zhang et al., 2023c; Chen et al., 2023a). It has been shown that straw return can effectively increase the DOC content in soil (Huang et al., 2024). In addition, the dissolved substances produced during straw decomposition have significantly altered the fluorescence composition of the original soil DOM (Tang et al., 2024a). Typically, straw return is combined with tillage practices. The depth of tillage affects the degree of straw-soil mixing, which in turn alters DOM characteristics in different soil layers (Latifmanesh et al., 2020; Huang et al., 2024). Studies have shown that the DOC content is higher under straw return with no-tillage treatment than under conventional tillage (Bu et al., 2020). However, straw mulching alone exerts a limited impact on DOM in the subsoil layers. Conventional and deep tillage have been suggested to facilitate more effective straw incorporation, potentially exerting greater influence on deep soil DOM characteristics (Zhao et al., 2023; Zhou et al., 2023; Huang et al., 2024). Subsurface soil layers (>20 cm) contain over 50 % of the total soil nutrients and organic matter, relying on DOM leaching as a critical nutrient source for microbial communities (Zosso et al., 2023; Jiang et al., 2024a). Different straw return treatments significantly affect the leaching process of DOM, which may alter the pattern of DOM fluorescent substance variations with soil depth and thus affect soil nutrient cycling (Liu et al., 2023a; Xiao et al., 2025). However, the mechanism through which different straw return treatments regulate the vertical distribution of SMQ by affecting DOM characteristics in different soil layers remains unclear, thereby impeding the formulation of rational agricultural management strategies.

A field experiment was designed with four treatments: conventional tillage (CT), no-tillage with straw mulch (NTS), conventional tillage with straw mulch and incorporation (CTS), and deep tillage with straw incorporation (DTS) to explore the relationship between DOM characteristics and SMQ. We hypothesized that: (1) straw return would significantly increase SMQ across all soil layers (0–40 cm), with the most significant enhancement under CTS and DTS; (2) different straw return treatments would alter DOM characteristics and their vertical distribution; and (3) SMQ enhancement via straw return would be primarily driven by changes in DOM characteristics, especially in the subsoil layers (>20 cm). This study elucidated the mechanism by which DOM regulates SMQ and provided a scientific basis for optimizing straw return strategies to improve soil quality.

2. Materials and methods

2.1. Study sites

The experimental site was situated in Chenjiadian Village ($44^{\circ}07'N$, $125^{\circ}14'E$), Changchun City, Jilin Province, Northeast China. The mean annual temperature in the region is $4.4^{\circ}C$, and the average annual precipitation is 550 mm. The soil is classified as Mollisols with a clay loam texture. Initial soil properties were as follows: pH, 6.3; SOC, 17.08 g kg^{-1} ; total nitrogen (TN), 1.45 g kg^{-1} ; available nitrogen (AN), 79.47 mg kg^{-1} ; available phosphorus (AP), 35.26 mg kg^{-1} ; and available potassium (AK), $150.13 \text{ mg kg}^{-1}$.

2.2. Experiment design and sample collection

A field experiment initiated in 2012 was conducted using a continuous maize cropping system. The area of each experimental plot was $45,000 \text{ m}^2$ ($450 \times 100 \text{ m}$). Four treatments were applied: (1) conventional tillage (CT) where the depth of tillage is 20 cm and straw is removed; (2) no-tillage with straw mulch (NTS), which involves no-tillage and straw mulching; (3) conventional tillage with straw mulch and incorporation (CTS), involving a 20 cm tillage depth, with 30 % of the straw mulching the soil surface and 70 % incorporated into the

0–20 cm layer; and (4) deep tillage with straw incorporation (DTS), featuring a tillage depth of 40 cm and full straw incorporation into the 30–40 cm layer. Within each treatment plot, four subplots were established using an S-shaped sampling strategy, and each subplot measured 16 m ($4 \text{ m} \times 4 \text{ m}$) and was separated by 100 m from adjacent subplots (Zhao et al., 2025). Following the autumn harvest, maize straw was fully returned to the field at approximately $11,000 \text{ kg ha}^{-1}$ after being cut into 5 cm pieces. The fertilizer inputs at spring seeding included 89 kg N ha^{-1} , $51 \text{ kg P}_2\text{O}_5 \text{ ha}^{-1}$, and $78 \text{ kg K}_2\text{O ha}^{-1}$, with an additional 89 kg N ha^{-1} applied at the jointing stage.

In August 2024, soil samples were collected using a random sampling method across four soil depth layers (0–10, 10–20, 20–30, and 30–40 cm) with four replicate samplings. Specifically, four soil core samples were collected from each depth layer, yielding 16 soil samples (4 depths \times 4 replicates) per subplot. After removing visible gravel and plant roots, samples from the same treatment plot and depth layer were thoroughly mixed to form composite samples. A portion of each composite sample was stored at 4°C for the subsequent analysis of enzyme activity and MBC, while the remaining portion was air-dried and screened through 0.25 mm mesh sieves for soil properties analysis and DOM extraction.

2.3. Soil properties and enzyme activity characterization

Soil pH (w/v = 1:5) was determined using a digital pH meter (PB-10, Sartorius, Germany). SOC and TN were measured using an elemental analyzer (EA3000, EuroVector, Italy). AN, AP, and AK were analyzed using the methodologies outlined in *Soil Agro-Chemical Analysis* (Bao, 2000). MBC was determined using the method of Chen et al. (2017). The activities of β -1,4-glucosidase (BG), acid phosphatase (ACP), L-leucine aminopeptidase (LAP), and β -1,4-N-acetylglucosaminidase (NAG) were quantified using a microplate fluorescence assay (Yang et al., 2024a).

2.4. DOM extraction and spectral analysis

6 g of air-dried soil ($\leq 0.25 \text{ mm}$) were mixed with 30 mL of Milli-Q water in a 50 mL centrifuge tube at a soil-to-water ratio of 1:5 (w/v) and shaken in the dark at 25°C and 200 rpm for 12 h (Wang et al., 2023a; Wu et al., 2023). The resulting suspensions were centrifuged at 25°C and $3500 \times g$ for 15 min using a centrifuge (Sorvall ST 16R, Germany), and the supernatants were subsequently filtered through a $0.45 \mu\text{m}$ cellulose membrane (Wang et al., 2024a; Jiang et al., 2024b). All DOM solutions were stored in the dark at 4°C for no more than 7 days. DOC was analyzed using a total organic carbon analyzer (Elementar Vario TOC cube, Germany).

For spectral analysis, the DOM solutions were diluted with Milli-Q water to a DOC of 6 mg C L^{-1} . Fluorescence excitation-emission matrix (EEM) spectroscopy was performed using a Hitachi fluorescence spectrophotometer (F-7100, Japan). The scanning speed was set to 1200 nm min^{-1} , with the excitation wavelengths ranging from 200 to 450 nm (5 nm intervals) and emission wavelengths from 250 to 600 nm (2 nm increments), 5 nm slit widths for both excitation and emission and a PMT voltage of 700 V (Yang et al., 2024b). Synchronous fluorescence spectroscopy (SFS) was conducted over a scanning range of 250–600 nm (5 nm increments) at a scanning speed of 240 nm min^{-1} with $\Delta\lambda = 18 \text{ nm}$ (Guo et al., 2019; Mu et al., 2022). Milli-Q water was used as the blank control. All spectra were corrected for background by subtracting Milli-Q water blanks and adjusting for inner-filter effects using the corresponding absorbance data.

2.5. Fluorescence spectral analysis

Parallel factor analysis (PARAFAC) was conducted utilizing MATLAB R2024a with the DOMFluor toolbox (<http://www.models.life.ku.dk>) on a dataset comprising 48 soil samples from all experimental treatments. After removing outliers, residual analysis and split-half analysis were

used to validate the optimal number of components. The identified fluorescent components were validated by comparison with the reference spectra available in the OpenFluor database (<https://openflour.lablicate.com/>). The maximum fluorescence intensities (Fmax) in relative units (R.U.) for each component were used to quantify their relative abundances. C1 + C2 and C3 + C4 represent the relative abundances of humic-like components and protein-like components, respectively. In addition, the humification index (HIX), biotic index (BIX), and fluorescence index (FI) were calculated from the corrected EEM data using the method described in the [supplemental material](#).

Two-dimensional correlation spectroscopy (2D-COS) was conducted using 2D-Shige software (Kwansei-Gakuin University, Japan) following the procedure described by [Chen et al. \(2019b\)](#). Based on Noda's rules, if the product of synchronous and asynchronous cross-peak intensities is positive, the variation in x_1 is greater than that of x_2 in the soil profile. Conversely, if the product is negative, x_2 varies more rapidly than x_1 ([Noda, 2012](#)).

2.6. Statistical analysis

SMQ was calculated by [Eq. \(1\)](#), where MBC is microbial biomass carbon (mg kg^{-1}) and SOC is soil organic carbon (g kg^{-1}).

$$\text{SMQ} = \frac{\text{MBC}}{\text{SOC}} \times 100\% \quad (1)$$

One-way ANOVA was used to evaluate significant differences among straw return treatments. The applicability of principal component analysis (PCA) was verified using the Kaiser-Meyer-Olkin (KMO) test and Bartlett's test of sphericity, which were conducted on SFS data using SPSS 26.0 (IBM, Chicago, IL, USA). The ChiPlot platform (<https://www.chiplot.online/>) was then used to perform PCA on the SFS data of DOM to characterize the DOM variations with soil depth. Redundancy analysis (RDA) was conducted utilizing Canoco 5 (CANOCO, NY, USA) to explore correlations among DOM characteristics, soil physicochemical

properties, and enzyme activities. Multiple linear regression and correlation analyses were performed using Origin 2021 to assess associations among SMQ, soil physicochemical properties, enzyme activities, and DOM characteristics. To identify key predictive factors of SMQ, the "randomForest" package in R (version 4.4.0) was used to construct a random forest model. Hyperparameters were optimized via grid search: mtry across {2, 3, 4, 5} (near the regression default mtry $\approx p/3$, where p = number of features) and ntree across {500, 1000, 1500} to balance model stability and computational efficiency. A 10-fold cross-validation was conducted to validate model performance.

3. Results

3.1. Changes in SMQ

DOC, MBC, and SOC concentrations exhibited a declining trend with soil depth ([Fig. 1](#)). Compared to the CT treatment, straw return increased all three carbon pools, although the DTS treatment significantly reduced their concentrations in the 0–10 cm layer by 5.23–7.12 %. The mean DOC concentrations followed the order NTS > CTS > DTS > CT, whereas the order for MBC and SOC was CTS > NTS > DTS > CT.

SMQ similarly decreased with depth ([Fig. 1d](#)). In the 0–10 cm layer, both the NTS and CTS treatments significantly increased SMQ, with the NTS treatment producing the greatest enhancement (15.69 %). In the 10–20 and 20–30 cm layers, CTS treatment yielded the highest improvements (9.02 % and 17.05 %, respectively). At the 30–40 cm layer, DTS treatment showed the greatest enhancement in SMQ (9.45 %). Across the 0–40 cm profile, the average SMQ values ranged from 1.66 % to 1.85 %, with the ranking: CTS > NTS > DTS > CT ([Fig. S2](#)). The SMQ decline rate in CT treatment was $0.014\% \text{ cm}^{-1}$, whereas NTS ($0.022\% \text{ cm}^{-1}$) and CTS ($0.019\% \text{ cm}^{-1}$) treatment accelerated this decline, while DTS treatment ($0.011\% \text{ cm}^{-1}$) decelerated it relative to CT treatment, reflecting divergent depth-response patterns among straw return

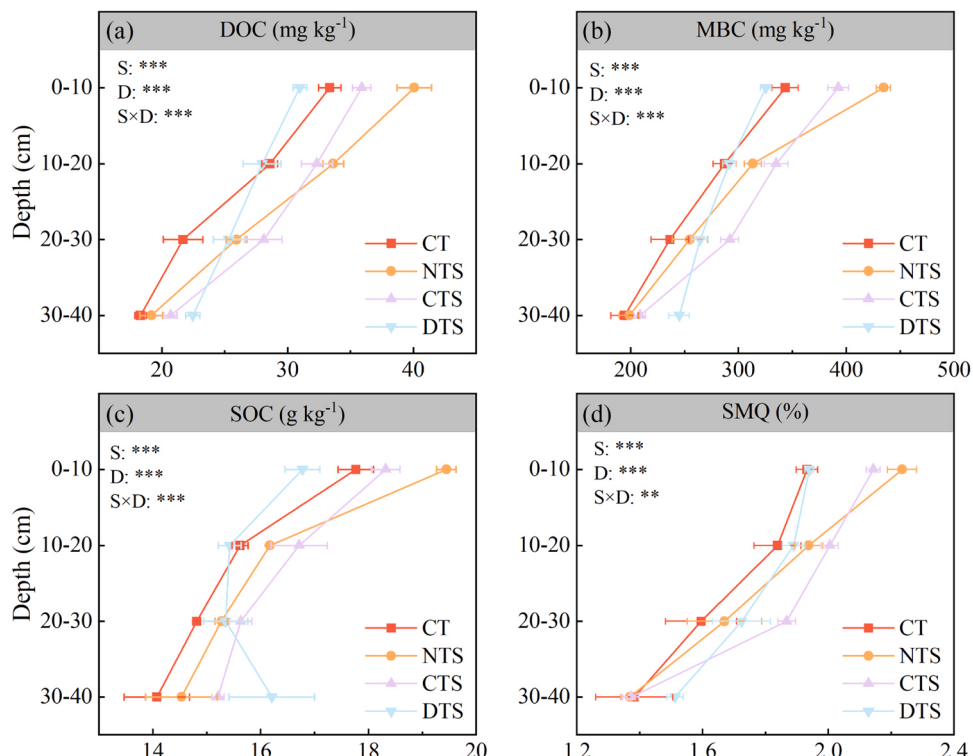


Fig. 1. Effects of straw return treatments on (a) DOC, (b) MBC, (c) SOC, and (d) SMQ. DOC, dissolved organic carbon; MBC, microbial biomass carbon; SOC, soil organic carbon; SMQ, soil microbial quotient; CT, conventional tillage; NTS, no-tillage with straw mulch; CTS, conventional tillage with straw mulch and incorporation; DTS, deep tillage with straw incorporation; S, straw return; D, soil depth; and S × D, interaction. * $P < 0.05$, ** $P < 0.01$, and *** $P < 0.001$.

treatments.

3.2. Changes in soil enzyme activities

Soil enzyme activities exhibited a consistent decline with soil depth (Fig. 2). Straw return significantly enhanced enzyme activities across all layers. In the 0–10 cm layer, both NTS and CTS treatments significantly increased the activities of BG, ACP, and NAG, with NTS demonstrating the greatest enhancement (12.50–39.67%). In contrast, DTS treatment significantly reduced enzyme activities in this layer by 6.42–12.89%. In the 10–20 and 20–30 cm layers, CTS treatment was the most effective, increasing activities of BG, ACP, LAP, and NAG by 5.86–40.29% and 6.51–60.31%, respectively. In the 30–40 cm layer, the highest enzyme activities were observed under DTS treatment, with increases of 7.96–53.62%. Overall, enzyme activity levels in the 0–40 cm soil profile followed the order: CTS > NTS > DTS > CT (Fig. S3).

3.3. EEM-PARAFAC of DOM

PARAFAC analysis identified four fluorescent DOM components (Fig. 3 and Fig. S4). Component 1 (C1), with excitation/emission (Ex/Em) wavelengths of 236/400 nm, was classified as microbial humic-like substance, typically derived from microbial processing (Chen et al., 2019a; Coulson et al., 2022). Component 2 (C2), characterized by Ex/Em = 262/455 nm, was identified as terrigenous humic-like substance, notable for its high aromaticity and low bioavailability (Dainard et al., 2019). Component 3 (C3), with Ex/Em wavelengths of 224 (278)/330 nm, was assigned to tryptophan-like substance, which was closely linked to microbial activity and metabolism (Paradina-Fernández et al., 2023). Component 4 (C4), with Ex/Em = 218 (268)/285 nm, was attributed to a tyrosine-like substance and was highly sensitive to microbial activity (Obrador et al., 2018; Wang et al., 2024c).

The Fmax values of all DOM components decreased with soil depth

(Fig. 3e). In the 0–10 and 10–20 cm layers (Fig. 3f), DOM fluorescence was dominated by C1 + C2, accounting for 66.01%–74.50% and 56.98–63.37% of the total, respectively. In contrast, C3 + C4 predominated in the 20–30 and 30–40 cm layers, comprising 49.77–59.98% and 53.16–62.70% of the total, respectively. Moreover, straw return increased the proportions of C3+C4. In the 0–10 cm layer, NTS treatment exhibited the most pronounced increase in C3+ C4 relative abundances (8.49%). In the 10–20 and 20–30 cm layers, CTS treatment had the greatest increases (4.43% and 10.12%, respectively). In the 30–40 cm layer, DTS treatment induced the highest enhancement (9.54%). The mean total Fmax in the 0–40 cm layer followed the order: CTS > NTS > DTS > CT (Fig. S5).

Both FI and BIX of soil DOM increased with soil depth (Fig. 4a, b). The FI values ranged from 1.52 to 1.74 across all treatments, suggesting a mixed allochthonous and autochthonous origin of DOM. In the 0–10 cm layer, only NTS treatment significantly increased FI by 6.49%. The humification index (HIX) exhibited a decreasing trend with soil depth, whereas straw return treatments increased HIX values (Fig. 4). In the 0–10 cm layer, the NTS treatment achieved the highest HIX increase (13.06%). In the 10–20 and 20–30 cm layers, CTS treatment showed the greatest increases (8.44% and 10.33%, respectively). In the 30–40 cm layer, DTS treatment resulted in the highest increase in HIX (8.36%). The mean HIX values for the 0–40 cm layer followed the order: CTS > NTS > DTS > CT (Fig. S5).

3.4. SFS and 2D-COS of DOM

The SFS of DOM exhibited one distinct peak and three broad shoulders (Fig. 5a, S6). The prominent peak located within the 260–300 nm range corresponded to protein-like fluorescence (PLF) substances, including tryptophan-like (TRLF) and tyrosine-like (TYLF) fluorescence substances (Lu et al., 2021). The first shoulder between 300 and 350 nm was associated with microbial humic-like fluorescence (MHLF) substances (Yu et al., 2024). The second shoulder spanning

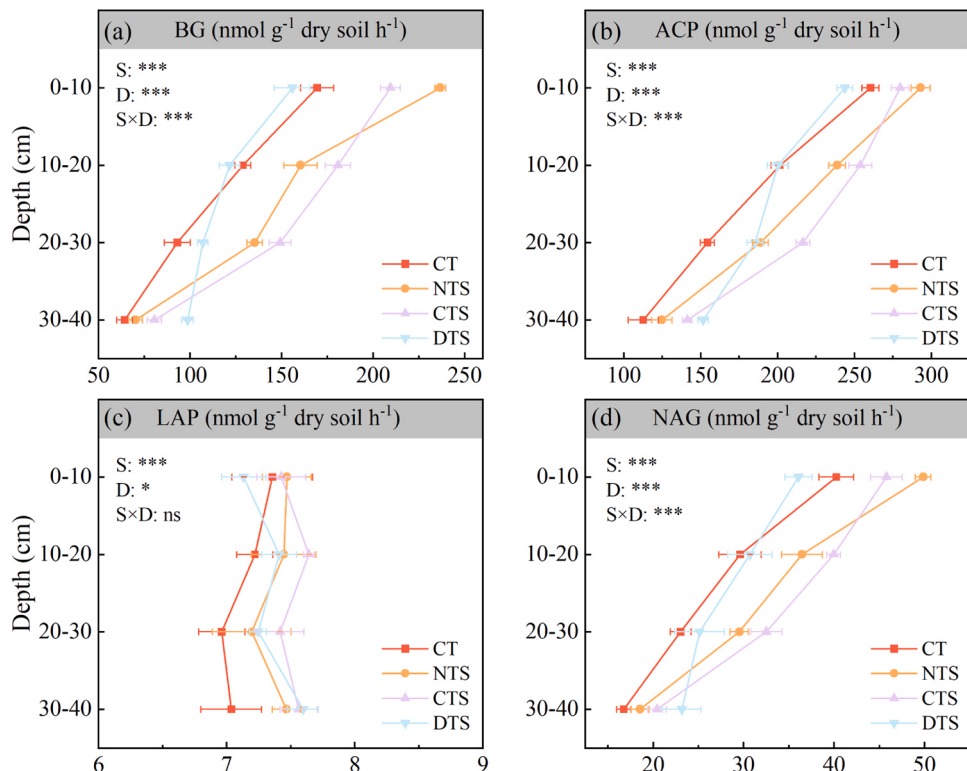


Fig. 2. Effects of straw return treatments on activities of (a) BG, (b) ACP, (c) LAP, and (d) NAG. BG, β -1,4-glucosidase; ACP, acid phosphatase; LAP, L-leucine aminopeptidase; NAG, β -1,4-N-acetylglucosaminidase.

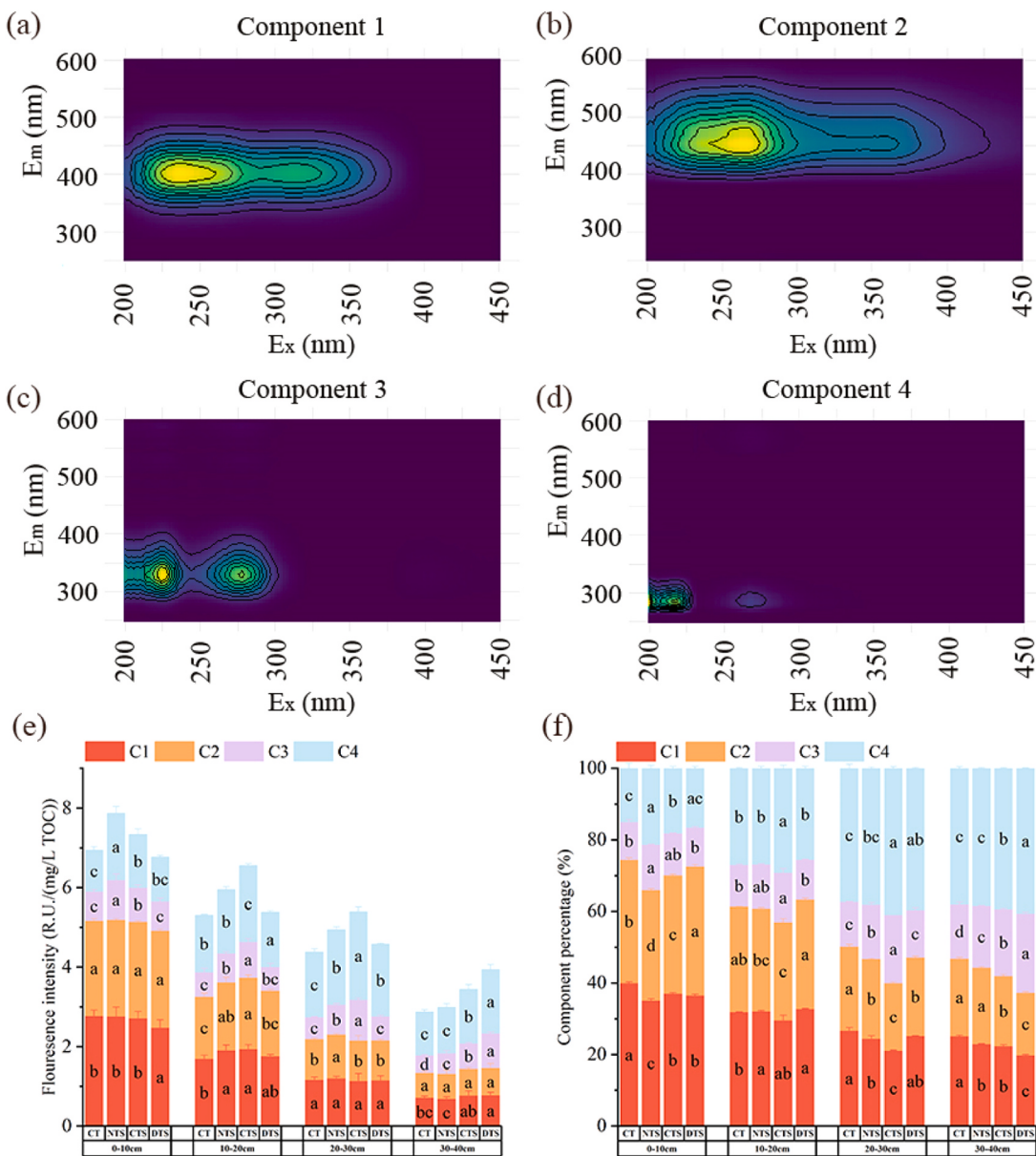


Fig. 3. PARAFAC identified (a–d) four DOM fluorescence components, (e) Fmax, and (f) relative abundances. Different letters indicate statistically significant differences. C1, microbial humic-like substance; C2, terrigenous humic-like substance; C3, tryptophan-like substance; C4, tyrosine-like substance.

350–460 nm was attributed to fulvic-like fluorescence (FLF) substances, whereas the third shoulder covering 460–600 nm represented humic-like fluorescence (HLF) substances (Liu et al., 2023a; Filep et al., 2024). The observed blue and red shifts in the SFS peaks indicated a notable spectral overlap among DOM fractions.

The KMO value was 0.911, and Bartlett's test of sphericity produced a p-value below 0.001, confirming the suitability of PCA. PCA of the SFS data extracted two principal components (PC1 and PC2). PC1 explained 99.92 % of the overall variance and exhibited one peak and two shoulders (Fig. 5b), with the peak at 280 nm corresponding to TRLF and the shoulders at 316 and 360 nm linked to MHLF and FLF, respectively. PC2 accounted for 0.05 % of the variance and displayed two weak shoulders (Fig. 5b). Shoulders at 262 and 467 nm were associated with TYLF and HLF, respectively. In the PCA loading plot (Fig. 5c), sample points from the 0–10 and 10–20 cm layers under straw return treatments formed distinct clusters that were separate from those under the CT treatment. This indicated that straw return significantly altered the DOM characteristics in those layers compared to the deeper layers

(20–30 and 30–40 cm).

2D-SFS-COS and hetero 2D-SFS-COS were applied to characterize the sequential variations in DOM fractions with soil depth. In the CT treatment (Fig. 6a, b), all fluorescence fractions in the synchronous spectra were positively correlated. In the asynchronous spectra, TRLF exhibited a positive correlation with TYLF, and the correlation trends between FLF and TRLF, as well as HLF and FLF, were consistent with those between TRLF and TYLF. However, HLF was negatively correlated with FLF. Therefore, the sequence of DOM fraction variation was determined as the order: MHLF → HLF → FLF → TRLF → TYLF. For the NTS treatment (Fig. 6c and d), the synchronous spectral patterns were consistent with those of the CT treatment. In the asynchronous spectra, MHLF and FLF were negatively correlated with TYLF. However, the correlation trends between FLF and TYLF, as well as between HLF and TRLF, were opposite to those observed between MHLF and TYLF. Accordingly, the variation sequence was determined as: MHLF → TYLF → FLF → TRLF → HLF. Under CTS treatment (Fig. 6e and f), the synchronous spectra revealed positive correlations among all DOM fractions, whereas the

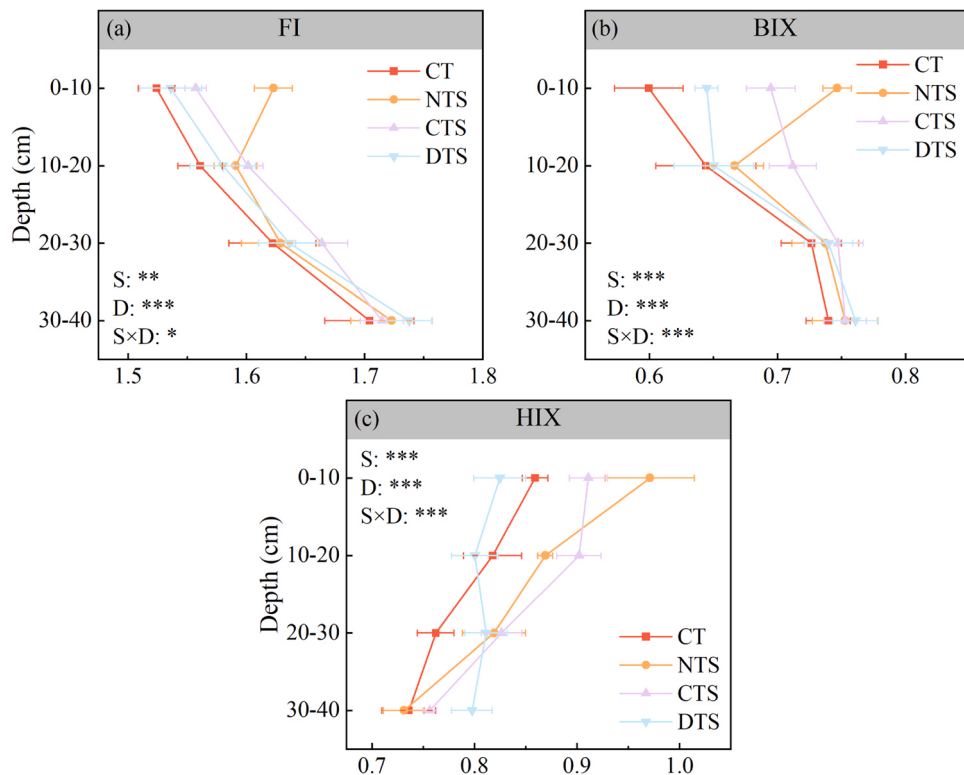


Fig. 4. Effects of straw return treatments on soil DOM (a) FI, (b) BIX, and (c) HIX. FI, fluorescence index; BIX, biological index; HIX, humification index.

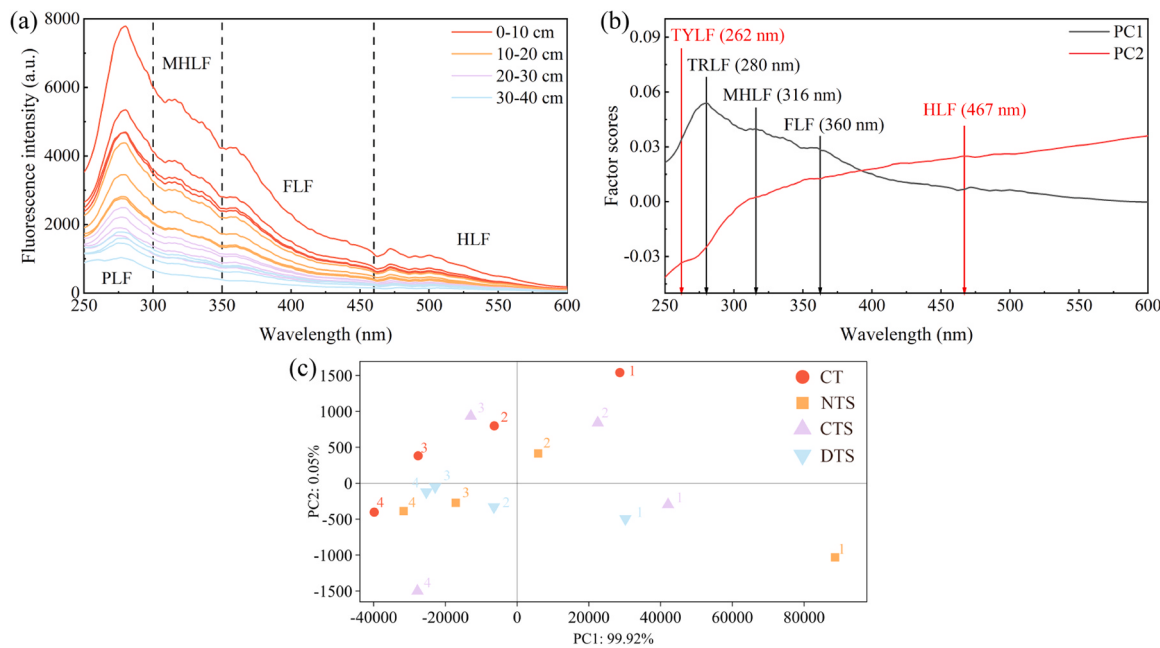


Fig. 5. (a) SFS of soil DOM under straw return treatments, (b) PC1 and PC2 score plots for spectral wavelengths, and (c) PC1 and PC2 loading plots for the soil sample dataset. PLF, protein-like fluorescent substances; MHLF, microbial humic-like fluorescent substances; TLF, fulvic-like fluorescent substances; HLF, humic-like fluorescent substances; 1, 0–10 cm; 2, 10–20 cm; 3, 20–30 cm; and 4, 30–40 cm.

asynchronous spectra exhibited negative cross-peaks. According to Noda's rules, the sequence was as follows: TLYL → TRLF → MHLF → FLF → HLF. For the DTS treatment (Fig. 6g and h), positive correlations were observed in the synchronous spectra for all DOM fractions. In the asynchronous spectra, positive correlations were identified between FLF and TLYL, MHLF and TRLF, and HLF and FLF, whereas MHLF and TLYL exhibited negative correlations. Thus, the variation sequence was

inferred as: HLF → FLF → TLYL → MHLF → TRLF.

3.5. Relationships among edaphic factors, enzyme activities, DOM characteristics, and SMQ

The first two axes of the RDA accounted for 80.58 % of the total variance in DOM characteristics (Fig. S7a). DOC and HIX were

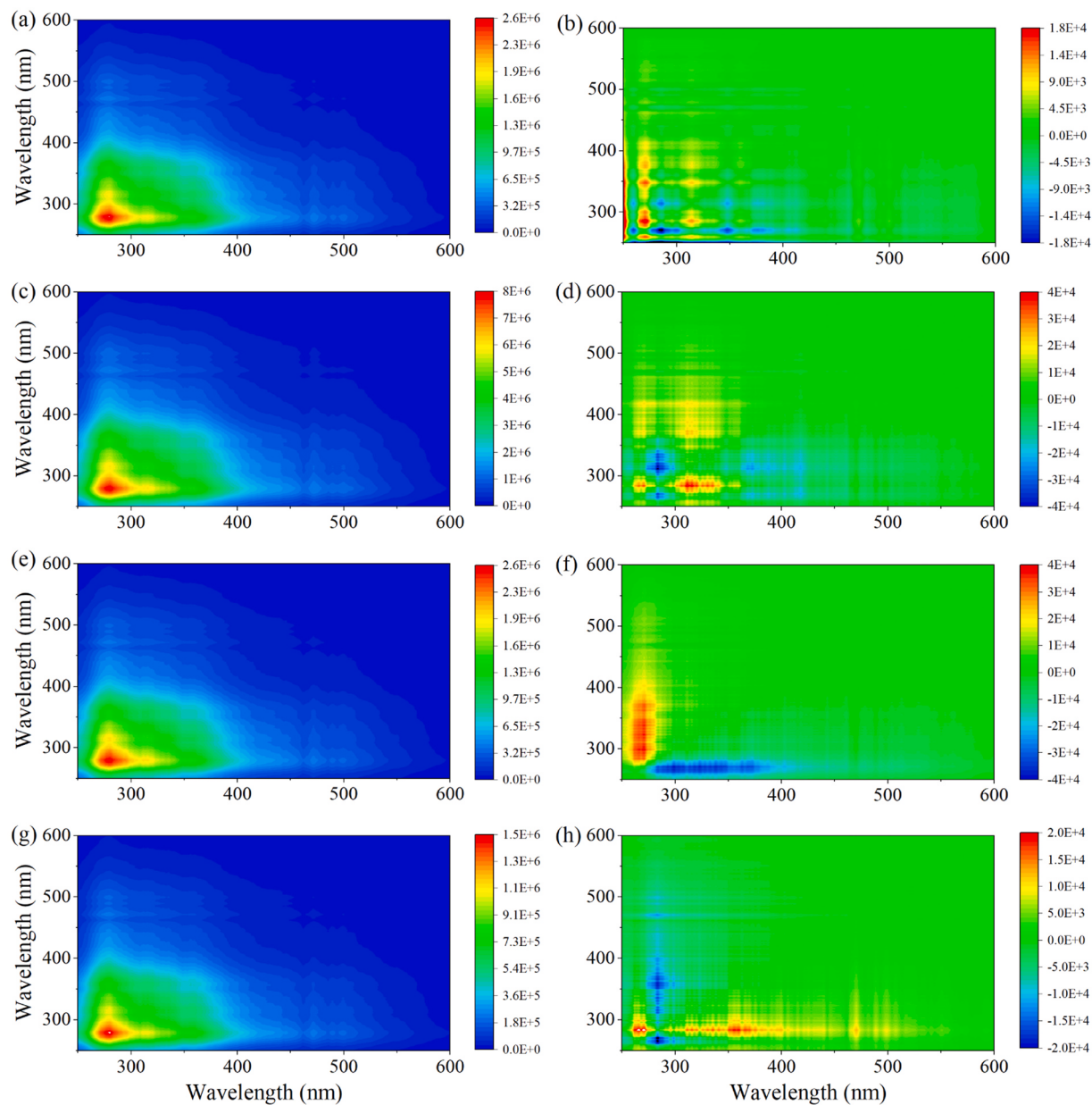


Fig. 6. Synchronous (a, c, e, g) and asynchronous (b, d, f, h) maps captured by 2D-SFS-COS of DOM components under different straw return treatments.

negatively correlated with soil pH and TN, whereas C1 + C2 showed a positive correlation with soil pH. Correlation analysis (Figs. S7b and S8) indicated that SMQ was negatively associated with pH and positively linked to other soil physicochemical parameters and enzyme activities. Linear regression analysis further demonstrated that SMQ was positively correlated with DOC and C1 + C2 (Fig. 7a), whereas negative correlations were observed with FI and BIX (Fig. 7d, e). Notably, in the DTS treatment, SMQ exhibited a negative relationship with C3 + C4, whereas in other treatments, it was positively correlated with HIX. Given the similarity in DOM characteristics between the 0–10 and 10–20 cm layers, and between the 20–30 and 30–40 cm layers, a random forest model was employed to assess the relative importance of factors influencing SMQ in the 0–20 and 20–40 cm layers. The R^2 values for the 0–20 and 20–40 cm layers were 0.77 and 0.70 (Fig. 8), respectively, with both root-mean-squared error and mean absolute error values less than 0.01 (Table S1), indicating a good model fit. Results showed that LAP, AP, and BG were the dominant regulators of SMQ in the 0–20 cm layer, whereas DOC and C1 + C2 were the primary drivers

in the 20–40 cm layer.

4. Discussion

4.1. Effects of straw return treatments on SMQ

Both MBC and SOC contents declined significantly with soil depth, which was consistent with the findings of Ding et al. (2025). These vertical patterns were primarily due to reduced inputs of plant residues and root exudates in subsurface layers (Pinheiro Alves de Souza et al., 2023; Tang et al., 2024b). Similarly, SMQ exhibited a decreasing trend with soil depth. This phenomenon can be explained by two factors: (1) limited permeability and suboptimal moisture conditions in deeper layers restrict microbial activity and biochemical processes (Cong et al., 2020); and (2) MBC was more strongly influenced by both biotic factors (e.g., enzyme activity and root distribution) and abiotic factors (e.g., pH, nutrient availability, and DOM characteristics) than SOC, thereby resulting in a more pronounced vertical reduction (Gao et al., 2024).

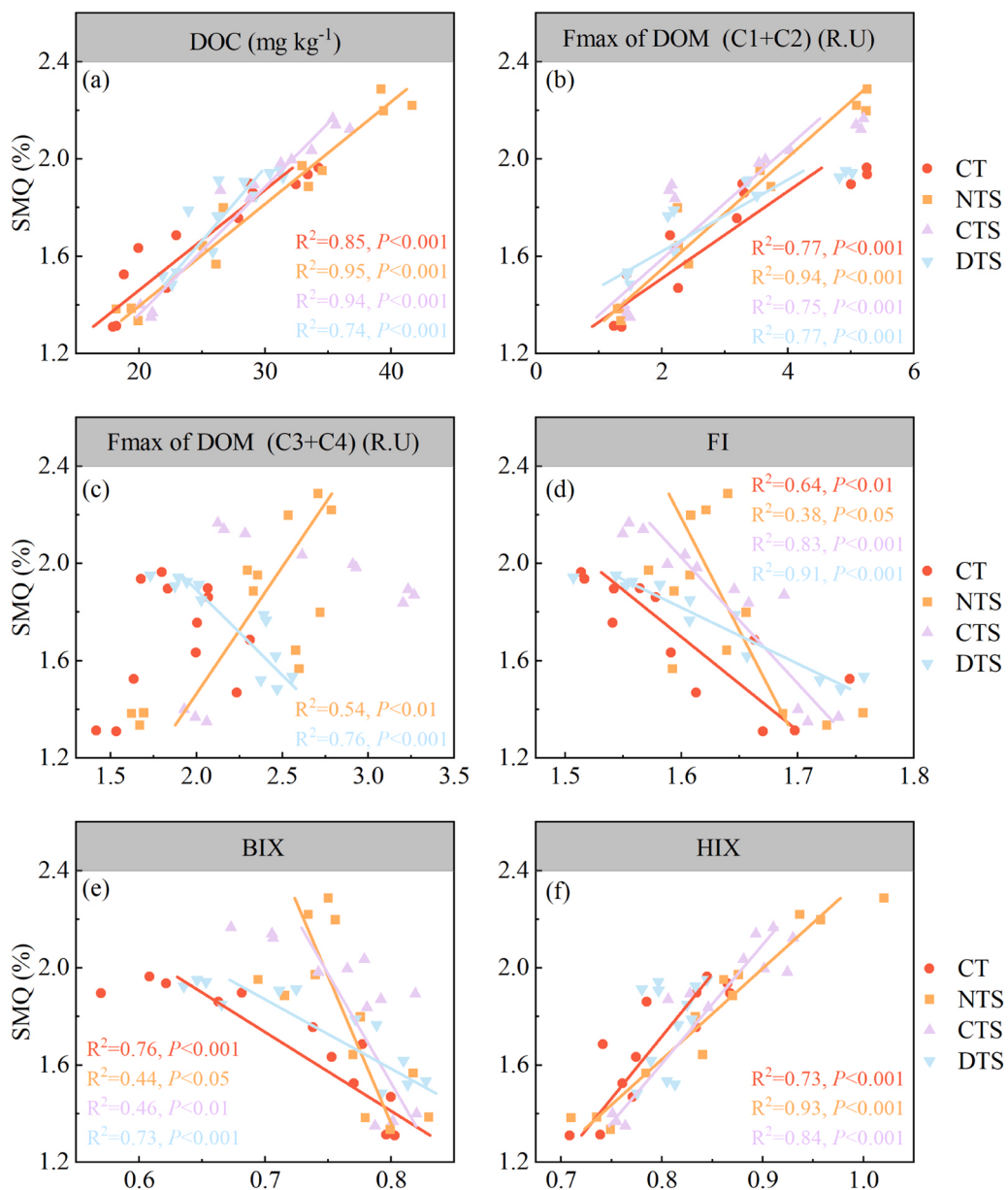


Fig. 7. SMQ correlation fitting with DOM characteristics under different straw return treatments.

The mean SMQ value in the 0–40 cm layer in this study was notably lower than the $3.56\% \pm 0.20\%$ reported by Sun et al. (2020b). This discrepancy could be attributable to the colder climate of the study region, which suppressed MBC levels compared with those in tropical and subtropical ecosystems (Hu et al., 2017). The application of straw return significantly enhanced MBC and SMQ in the 0–40 cm layer, indicating its effectiveness in stimulating microbial activity and improving soil quality (Chen et al., 2022). This is because the returned straw provided essential nutrients for microbial communities, stimulated the production of root exudates, and created favorable conditions for microbial processes and biochemical reactions (Sun et al., 2020a; Ding et al., 2023). Additionally, organic acids, such as glutamic acid and malic acid, released during straw decomposition may inhibit microbial community shifts towards copiotrophic life strategies, thereby promoting the proliferation of functional microorganisms and contributing to increased SMQ (Yan et al., 2022; Liang et al., 2023).

Previous reports have shown the effectiveness of NTS treatment in maintaining microbial activity and enhancing SMQ (Chen et al., 2022). Our results demonstrated a more substantial improvement in SMQ under

CTS treatment. This discrepancy may be attributed to differences in the soil depth ranges investigated. Although NTS treatment significantly enhanced SMQ in the 0–10 cm layer, its effect decreased with soil depth (Liu et al., 2025). In contrast, CTS treatment facilitated more uniform straw-microbe interactions across the 0–10 and 10–20 cm layers by evenly distributing straw, thereby promoting straw decomposition and increasing MBC content (Latifmanesh et al., 2020). In comparison, DTS treatment concentrated straw incorporation in the 30–40 cm layer, leading to negligible improvements in SMQ within the upper 0–30 cm layer. In addition, deep tillage-induced disturbance mixed nutrients from the 0–10 cm layer into deeper layers, resulting in lower MBC and SOC in this layer compared to the CT treatment (Thapa et al., 2023).

The results confirmed hypothesis (1), indicating that straw return significantly enhanced SMQ across the 0–40 cm layer, with the most pronounced effect under CTS treatment. Notably, the effects of different straw return treatments on SMQ in deeper layers (>40 cm) were not analyzed in this study. Future studies should investigate the effects of different straw return treatments on SMQ in soil layers below 40 cm to elucidate the vertical differentiation mechanism underlying SMQ

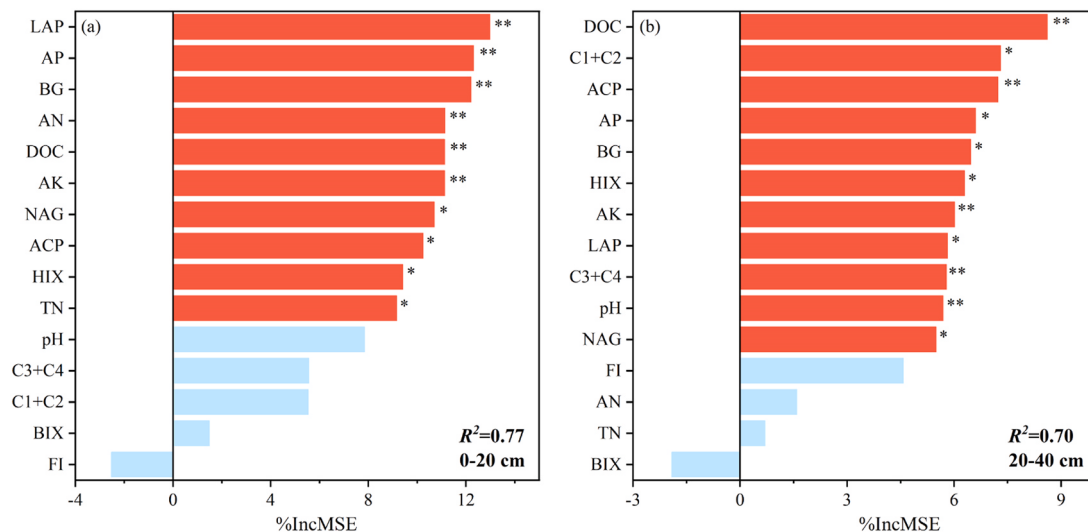


Fig. 8. Random Forest analysis of the relative importance of factors influencing SMQ in the (a) 0–20 cm and (b) 20–40 cm layer under different straw return treatments.

enhancement.

4.2. Effects of straw return treatments on DOM characteristics

Increasing soil depth was accompanied by higher FI and BIX values, which were consistent with the findings of Wang et al. (2024d), indicating a stronger contribution from microbial sources (Kaiser and Kalbitz, 2012). The 0–20 cm layer exhibited greater DOM humification than the 20–40 cm layer, in contrast to Romero et al. (2017), who observed an increase in HIX with soil depth. This difference may be due to differences in cropping systems. The higher TN content in legume-cereal rotation systems promoted microbial utilization of humic-like DOM components, thereby reducing HIX in surface layers compared to deeper soils (Yang et al., 2024c). While straw return could increase the relative proportion of humic-like components (Zhang et al., 2024), a decline in the percentage of C1 + C2 components was observed in the present study. This discrepancy is probably attributed to differences in decomposition stages. During the early stages of decomposition, protein-like components dominate the DOM pool (Cheng et al., 2024). In contrast, the proportion of humic-like components increases in the later stages (Wahdan et al., 2023).

In EEM spectra, the overlap between FLF and HLF limited their effective separation (Niloy et al., 2022; Li et al., 2023). As a result, EEM-PARAFAC identified only four fluorescent components, whereas PCA resolved five components. Straw return significantly altered the dynamic patterns of DOM fractions. In the CT treatment, MHLF and FLF displayed greater vertical variation than TRLF, indicating that soil organic matter was microbially humified and converted into more stable forms (Mielnik et al., 2021). Under NTS and CTS treatments, MHLF and TYLF exhibited greater vertical variation than HLF and FLF, suggesting that a substantial portion of the straw was decayed by microorganisms (Zhang et al., 2023c). Under DTS treatment, fungi and actinomycetes in the 30–40 cm layer resulted in more conversion of straw into humic-like substances, which accelerated the vertical variation order in HLF and FLF (Song et al., 2022b).

RDA indicated that DOC and HIX exhibited a negative correlation with soil pH while demonstrating positive correlations with other soil physicochemical properties and enzyme activities. This pattern may be attributed to the low soil pH in the study region, which promotes the prevalence of acid-tolerant microbial communities, particularly fungi (Aciego Pietri and Brookes, 2009). In contrast, C1 + C2 exhibited a positive correlation with soil pH, which may be explained by the increased solubility of humic-like substances at higher pH levels (Wang

et al., 2023b). This result is in line with previous research indicating that elevated soil pH can enhance the solubilization of C1 + C2 while reducing the concentrations of C3 + C4 (Li et al., 2018).

The results confirmed hypothesis (2), demonstrating that straw return significantly influenced the characteristics of DOM and the dynamic variations of its fractions with soil depth. However, because only a single sampling period was included in this study, the temporal dynamics of DOM characteristics under straw return treatments could not be fully captured.

4.3. Effects of DOM on SMQ

Linear regression analysis indicated that SMQ was positively associated with DOC and C1 + C2 while exhibiting negative correlations with FI and BIX under straw return treatments. These results may be attributed to the following factors: (1) DOC, as a crucial and labile carbon source for microorganisms, effectively enhances microbial activity, thereby increasing SMQ (Sui et al., 2025); (2) the slower decomposition of C1 + C2 reduces microbial metabolic quotient, which facilitates long-term SMQ stabilization (Yang et al., 2024c); and (3) the lower FI and BIX values reflect more stable terrestrial DOM inputs, which serve as sustained carbon sources for microbial communities (Hou et al., 2024).

In NTS treatment, favorable aeration and nutrient conditions promoted r-strategy microorganisms as dominant taxa in straw degradation. This treatment's higher proportion of protein-like components further enhanced microbial activity, significantly boosting SMQ (Li et al., 2023; Huang et al., 2024). In particular, the sequence of higher TYLF and TRLF variations in NTS and CTS treatments may further increase microbial activity, establishing positive feedback for SMQ enhancement (Gong et al., 2021; Liu et al., 2023b). In contrast, the DTS treatment concentrated straw in the 30–40 cm layer. The low-oxygen and nutrient-limited environment in this layer favored the dominance of K-strategy microorganisms (Filep et al., 2022). Accumulation of C3 + C4 components in this layer may activate r-strategy microorganisms in the short term but inhibit K-strategy microorganisms, thus being detrimental to the sustainable enhancement of deep soil SMQ (Chen et al., 2023b; Zhang et al., 2023b). Notably, HLF and FLF showed higher variations under DTS treatment, which may decrease microbial metabolic quotient and thus increase SMQ. This treatment difference led to a positive correlation between SMQ and C3 + C4 under NTS treatment, while an opposite correlation was observed under DTS treatment.

In the 0–20 cm layer, straw return created a favorable

microenvironment for microorganisms, stimulating their activities and increasing nutrient demands (Sun et al., 2020b; Dai et al., 2021). Therefore, soil enzyme activities and nutrients were the primary regulators of SMQ in the 0–20 cm layer. With increasing depth, inputs of plant residues and root exudates decreased, and the microbial community in the 20–40 cm layer primarily relied on DOM leaching for energy, highlighting DOM characteristics as key determinants of SMQ in subsurface layers (Gao et al., 2022). These results confirmed hypothesis (3): straw return could enhance SMQ mainly by modifying DOM characteristics, particularly in the 20–40 cm layer.

5. Conclusion

This study revealed how DOM characteristics regulated SMQ under straw return treatments. In the 0–40 cm layer, SMQ decreased with soil depth. Straw return significantly increased SMQ, and DTS treatment slowed SMQ decline, whereas NTS and CTS treatments accelerated it. Compared with CT, NTS and CTS accelerated the variation of protein-like fluorescent substances with soil depth, whereas DTS promoted humic-like fluorescent substances, thereby increasing SMQ. In the 0–20 cm layer, soil enzyme activities (LAP and BG) and nutrients (AP and AN) were the primary drivers of SMQ, while DOM characteristics (DOC and C1 + C2) regulated SMQ dynamics in the 20–40 cm layer. These findings underscore the regulatory role of DOM in SMQ improvement and provide a scientific basis for refining straw return strategies to promote soil health in Northeast China and similar agro-ecosystems around the world.

CRediT authorship contribution statement

Wei Yang: Writing – original draft, Software, Methodology, Investigation, Formal analysis, Conceptualization. **Yuanchen Zhu:** Writing – original draft, Software, Methodology, Investigation, Formal analysis, Conceptualization. **Wenxu Zou:** Writing – review & editing, Supervision, Resources, Funding acquisition, Conceptualization. **Xiaozeng Han:** Visualization, Investigation. **Jie Su:** Visualization, Investigation. **Zhimin Wu:** Visualization, Investigation. **Ying Zhao:** Visualization, Software, Investigation. **Yue Jiang:** Software, Methodology, Investigation, Data curation. **Juanjuan Qu:** Writing – original draft, Software, Methodology, Investigation, Data curation.

Declaration of Competing Interest

The authors declare that they have no known competing financial interests or personal relationships that could have appeared to influence the work reported in this paper.

Acknowledgments

We thank Aizhen Liang from the Northeast Institute of Geography and Agroecology, Chinese Academy of Sciences, for her help in experimental design and soil sampling. This research was supported by the National Key R & D Program of China (2022YFD1500100), the Outstanding Youth Fund of Heilongjiang Province (JQ2024D002), the by China Agriculture Research System of MOF and MARA (CARS04), the Chunyan Support program of Technology Talent of Heilongjiang Province (CYCX24026), and the China Postdoctoral Science Foundation (2023M743475).

Appendix A. Supporting information

Supplementary data associated with this article can be found in the online version at doi:10.1016/j.agee.2025.109840.

Data availability

Data will be made available on request.

References

- Aciego Pietri, J.C., Brookes, P.C., 2009. Substrate inputs and pH as factors controlling microbial biomass, activity and community structure in an arable soil. *Soil Biol. Biochem.* 41, 1396–1405.
- Bao, S., 2000. Soil Agrochemical Analysis. China Agricultural Press, Beijing.
- Bhaduri, D., Sih, D., Bhownik, A., Verma, B.C., Munda, S., Dari, B., 2022. A review on effective soil health bio-indicators for ecosystem restoration and sustainability. *Front. Microbiol.* 13, 938481.
- Bu, R., Ren, T., Lei, M., Liu, B., Li, X., Cong, R., Zhang, Y., Lu, J., 2020. Tillage and straw returning practices effect on soil dissolved organic matter, aggregate fraction and bacteria community under rice-rice-rape seed rotation system. *Agric. Ecosyst. Environ.* 287, 106681.
- Chen, S., Lu, Y., Dash, P., Das, P., Li, J., Capps, K., Majidzadeh, H., Elliott, M., 2019a. Hurricane pulses: Small watershed exports of dissolved nutrients and organic matter during large storms in the Southeastern USA. *Sci. Total Environ.* 689, 232–244.
- Chen, Y., Sui, W., Wang, J., He, D., Dong, L., Wanek, J.J., Wang, F., 2023b. Refractory humic-like dissolved organic matter fuels microbial communities in deep energy-limiting marine sediments. *Sci. China Earth Sci.* 66 (8), 1738–1756.
- Chen, L., Sun, S., Zhou, Y., Zhang, B., Peng, Y., Zhuo, Y., Ai, W., Gao, C., Wu, B., Liu, D., Sun, C., 2023a. Straw and straw biochar differently affect fractions of soil organic carbon and microorganisms in farmland soil under different water regimes. *Environ. Technol. Innov.* 32, 103412.
- Chen, W., Teng, C.Y., Qian, C., Yu, H.Q., 2019b. Characterizing properties and environmental behaviors of dissolved organic matter using two-dimensional correlation spectroscopic analysis. *Environ. Sci. Technol.* 53 (9), 4683–4694.
- Chen, Z., Wang, H., Liu, X., Zhao, X., Lu, D., Zhou, J., Li, C., 2017. Changes in soil microbial community and organic carbon fractions under short-term straw return in a rice-wheat cropping system. *Soil Till. Res.* 165, 121–127.
- Chen, W., Yuan, W., Wang, J., Wang, Z., Zhou, L., Liu, S., 2022. No-tillage combined with appropriate amount of straw returning increased soil biochemical properties. *Sustainability* 14 (9), 4875.
- Cheng, Z., Hu, Q., Guo, H., Ma, Q., Zhou, J., Wang, T., Zhu, L., 2024. Long-term straw return enhanced the chlorine reactivity of soil DOM: Highlighting the molecular-level activity and transformation trade-offs. *Sci. Total Environ.* 951, 175485.
- Cong, P., Wang, J., Li, Y., Liu, N., Dong, J., Pang, H., Zhang, L., Gao, Z., 2020. Changes in soil organic carbon and microbial community under varying straw incorporation strategies. *Soil Till. Res.* 204, 104735.
- Coulson, L.E., Weigelhofer, G., Gill, S., Hein, T., Griebler, C., Schelker, J., 2022. Small rain events during drought alter sediment dissolved organic carbon leaching and respiration in intermittent stream sediments. *Biogeochemistry* 159 (2), 159–178.
- Dai, W., Wang, J., Fang, K., Cao, L., Sha, Z., Cao, L., 2021. Wheat straw incorporation affecting soil carbon and nitrogen fractions in Chinese paddy soil. *Agriculture* 11 (8), 803.
- Dainard, P.G., Guéguen, C., Yamamoto-Kawai, M., Williams, W.J., Hutchings, J.K., 2019. Interannual variability in the absorption and fluorescence characteristics of dissolved organic matter in the Canada basin polar mixed waters. *J. Geophys. Res. Oceans* 124 (7), 5258–5269.
- Ding, W., Chen, J., Wu, Y., Mu, J., Qi, Z., Zvomuya, F., He, H., 2024. Responses of soil organic carbon, microbial biomass carbon, and microbial quotient to ground cover management practices in Chinese orchards: a data synthesis. *Plant Soil.* <https://doi.org/10.1007/s11104-024-07015-9>.
- Ding, H., Hu, Q., Cai, M., Cao, C., Jiang, Y., 2022. Effect of dissolved organic matter (DOM) on greenhouse gas emissions in rice varieties. *Agric. Ecosyst. Environ.* 330, 107870.
- Ding, W., Sun, L., Fang, Y., Zvomuya, F., Liu, X., He, H., 2025. Depth-driven responses of soil organic carbon fractions to orchard cover crops across China: a meta-analysis. *Soil Till. Res.* 246, 106348.
- Ding, Y., Wang, D., Zhao, G., Chen, S., Sun, T., Sun, H., Wu, C., Li, Y., Yu, Z., Li, Y., Chen, Z., 2023. The contribution of wetland plant litter to soil carbon pool: decomposition rates and priming effects. *Environ. Res.* 224, 115575.
- Filep, T., Zacháry, D., Jakab, G., Szalai, Z., 2022. Chemical composition of labile carbon fractions in Hungarian forest soils: Insight into biogeochemical coupling between DOM and POM. *Geoderma* 419, 115867.
- Filep, T., Zacháry, D., Ringer, M., Jakab, G., Bidló, Á., Szalai, Z., 2024. Applying fluorescence and 2D-correlation spectroscopy to elucidate changes in the chemical composition of DOM from soils with different vegetation types. *Arch. Agron. Soil Sci.* 70 (1), 1–14.
- Gao, J., Liu, L., Shi, Z., Lv, J., 2022. Characteristics of fluorescent dissolved organic matter in paddy soil amended with crop residues after column (0–40 cm) leaching. *Front. Environ. Sci.* 10, 766795.
- Gao, D., Shi, W., Wang, H., Liu, Z., Jiang, Q., Lv, W., Wang, S., Zhang, Y.L., Zhao, C., Hagedorn, F., 2024. Contrasting global patterns of soil microbial quotients of carbon, nitrogen, and phosphorus in terrestrial ecosystems. *Catena* 243, 108145.
- Gong, B., Zhong, X., Chen, X., Li, S., Hong, J., Mao, X., Liao, Z., 2021. Manipulation of composting oxygen supply to facilitate dissolved organic matter (DOM) accumulation which can enhance maize growth. *Chemosphere* 273, 129729.
- Guo, X.J., He, X.S., Li, C.W., Li, N.X., 2019. The binding properties of copper and lead onto compost-derived DOM using Fourier-transform infrared, UV-vis and

- fluorescence spectra combined with two-dimensional correlation analysis. *J. Hazard. Mater.* 365, 457–466.
- Hou, J., Li, J., Liu, D., Yu, H., Gao, H., Wu, F., 2024. Advancing fluorescence tracing with 3D-2D spectral conversion: a mixed culture on microbial degradation mechanisms of DOM from a large-scale watershed. *Environ. Res.* 262, 119877.
- Hu, Y., Wang, Z., Wang, Q., Wang, S., Zhang, Z., Zhang, Z., Zhao, Y., 2017. Climate change affects soil labile organic carbon fractions in a Tibetan alpine meadow. *J. Soils Sediment.* 17 (2), 326–339.
- Huang, R., Li, Z., Xiao, Y., Liu, J., Jiang, T., Deng, O., Tang, X., Wu, Y., Tao, Q., Li, Q., Luo, Y., Gao, X., Wang, C., Li, B., 2024. Composition of DOM along the depth gradients in the paddy field treated with crop straw for 10 years. *J. Environ. Manag.* 353, 120084.
- Jiang, P., Wan, X., Che, M.X., Chen, J.P., Liu, M.X., 2024a. Vegetation types shape the vertical distribution of dissolved organic matter in a mountainous soil. *Eurasia Soil Sci.* 57 (11), 1965–1975.
- Jiang, Y., Yang, W., Zhang, J., Liu, X., Jin, Y., Li, S., Qu, J., Wang, W., 2024b. Comparison of Pb adsorption and transformation behavior induced by chicken manure and its DOM in contaminated soil. *J. Environ. Chem. Eng.* 12, 114327.
- Kaiser, K., Kalbitz, K., 2012. Cycling downwards – dissolved organic matter in soils. *Soil Biol. Biochem.* 52, 29–32.
- Latifmanesh, H., Deng, A., Li, L., Chen, Z., Zheng, Y., Bao, X., Zheng, C., Zhang, W., 2020. How incorporation depth of corn straw affects straw decomposition rate and C&N release in the wheat-corn cropping system. *Agric. Ecosyst. Environ.* 300, 107000.
- Li, W., Li, X., Han, C., Gao, L., Wu, H., Li, M., 2023. A new view into three-dimensional excitation-emission matrix fluorescence spectroscopy for dissolved organic matter. *Sci. Total Environ.* 855, 158963.
- Li, X.M., Sun, G.X., Chen, S.C., Fang, Z., Yuan, H.Y., Shi, Q., Zhu, Y.G., 2018. Molecular chemodiversity of dissolved organic matter in paddy soils. *Environ. Sci. Technol.* 52 (3), 963–971.
- Liang, F., Li, B., Vogt, R.D., Mulder, J., Song, H., Chen, J., Guo, J., 2023. Straw return exacerbates soil acidification in major Chinese croplands. *Resour. Conserv. Recycl.* 198, 107176.
- Liu, H., Banfield, C., Gomes, S.I.F., Gube, M., Weig, A., Pausch, J., 2023b. Vegetation transition from meadow to forest reduces priming effect on SOM decomposition. *Soil Biol. Biochem.* 184, 109123.
- Liu, D., Hao, Y., Gao, H., Yu, H., Li, Q., 2023a. Applying synchronous fluorescence spectra with Gaussian band fitting and two-dimensional correlation to characterize structural composition of DOM from soils in an aquatic-terrestrial ecotone. *Sci. Total Environ.* 859, 160081.
- Liu, C., Si, B., Zhao, Y., Wu, Z., Lu, X., Chen, X., Han, X., Zhu, Y., Zou, W., 2025. Drivers of soil quality and maize yield under long-term tillage and straw incorporation in Mollisols. *Soil Till. Res.* 246, 106360.
- Lu, K., Xu, W., Yu, H., Gao, H., Gao, X., Zhu, N., 2021. Insight into temporal-spatial variations of DOM fractions and tracing potential factors in a brackish-water lake using second derivative synchronous fluorescence spectroscopy and canonical correlation analysis. *Environ. Sci. Eur.* 33 (1), 92.
- Mielnik, L., Hewelke, E., Weber, J., Oktaba, L., Jonczak, J., Podlasinski, M., 2021. Changes in the soil hydrophobicity and structure of humic substances in sandy soil taken out of cultivation. *Agric. Ecosyst. Environ.* 319, 107554.
- Mu, S., Sun, D., Liu, Y., Li, J., Zhang, H., Wang, J., 2022. Ultraviolet-visible and fluorescence spectra indicate the binding and transformation properties of hexavalent chromium in DOM solution. *J. Environ. Chem. Eng.* 10, 107158.
- Niloy, N.M., Shammi, M., Haque, Md.M., Tareq, S.M., 2022. Biogeochemistry of the dissolved organic matter (DOM) in the estuarine rivers of Bangladesh–Sundarbans under different anthropogenic influences. *Helyon* 8 (8), e10228.
- Noda, I., 2012. Close-up view on the inner workings of two-dimensional correlation spectroscopy. *Vib. Spectrosc.* 60, 146–153.
- Obrador, B., von Schiller, D., Marcé, R., Gómez-Gener, L., Koschorreck, M., Borrego, C., Catalán, N., 2018. Dry habitats sustain high CO₂ emissions from temporary ponds across seasons. *Sci. Rep.* 8 (1), 3015.
- Paradina-Fernández, L., Wünsch, U., Bro, R., Murphy, K., 2023. Direct measurement of organic micropollutants in water and wastewater using fluorescence spectroscopy. *ACS ES&T Water* 3 (12), 3905–3915.
- Romero, C.M., Engel, R.E., D'Andrilli, J., Chen, C., Zabinski, C., Miller, P.R., Wallander, R., 2017. Bulk optical characterization of dissolved organic matter from semiarid wheat-based cropping systems. *Geoderma* 306, 40–49.
- Song, D., Dai, X., Guo, T., Cui, J., Zhou, W., Huang, S., Shen, J., Liang, G., He, P., Wang, X., Zhang, S., 2022a. Organic amendment regulates soil microbial biomass and activity in wheat-maize and wheat-soybean rotation systems. *Agric. Ecosyst. Environ.* 333, 107974.
- Song, X., Zhao, M., Chen, A., Xie, X., Yang, H., Zhang, S., Wei, Z., Zhao, Y., 2022b. Effects of input of terrestrial materials on photodegradation and biodegradation of DOM in rivers: the case of Heilongjiang River. *J. Hydrol.* 609, 127792.
- de Souza, Pinheiro Alves, Schloter, Y., Weisser, M., Schulz, S.W., 2023. Deterministic development of soil microbial communities in disturbed soils depends on microbial biomass of the bioinoculum. *Microb. Ecol.* 86 (4), 2882–2893.
- Sui, X., Bao, X., Xie, H., Ba, X., Yu, Y., Yang, Y., He, H., Liang, C., Zhang, X., 2025. Contrasting seasonal effects of legume and grass cover crops as living mulch on the soil microbial community and nutrient metabolic limitations. *Agric. Ecosyst. Environ.* 380, 109374.
- Sun, T., Wang, Y., Hui, D., Jing, X., Feng, W., 2020b. Soil properties rather than climate and ecosystem type control the vertical variations of soil organic carbon, microbial carbon, and microbial quotient. *Soil Biol. Biochem.* 148, 107905.
- Sun, C., Wang, D., Shen, X., Li, C., Liu, J., Lan, T., Wang, W., Xie, H., Zhang, Y., 2020a. Effects of biochar, compost and straw input on root exudation of maize (*Zea mays L.*): from function to morphology. *Agric. Ecosyst. Environ.* 297, 106952.
- Tang, C., Hou, J., Liu, D., Xi, B., Li, J., Yu, H., 2024a. Applying fluorescence spectroscopy coupled with Gaussian band fitting to reveal dynamic variation process of humus fractions from riparian soils along an urbanized river. *Sci. Total Environ.* 927, 172193.
- Tang, H., Li, C., Shi, L., Wen, L., Li, W., Cheng, K., Xiao, X., 2024b. Tillage with crop residue returning management increases soil microbial biomass turnover in the double-cropping rice fields of Southern China. *Agronomy* 14 (2), 265.
- Thapa, V.R., Ghimire, R., Paye, W.S., VanLeeuwen, D., 2023. Soil organic carbon and nitrogen responses to occasional tillage in a continuous no-tillage system. *Soil Till. Res.* 227, 105619.
- Wahdan, S.F.M., Ji, L., Schädler, M., Wu, Y.T., Sansupa, C., Tanunchai, B., Buscot, F., Purahong, W., 2023. Future climate conditions accelerate wheat straw decomposition alongside altered microbial community composition, assembly patterns, and interaction networks. *ISME J.* 17 (2), 238–251.
- Wang, S., Heal, K.V., Zhang, Q., Yu, Y., Tigabu, M., Huang, S., Zhou, C., 2023a. Soil microbial community, dissolved organic matter and nutrient cycling interactions change along an elevation gradient in subtropical China. *J. Environ. Manag.* 345, 118793.
- Wang, Y., Hu, H., Zhou, Y., Zhang, B., Li, S., Liu, J., Tong, X., 2024c. Evolving characteristics of dissolved organic matter in soil profiles during 56 years of revegetation in Mu Us Sandy Land. *Plant Soil* 497 (1), 567–584.
- Wang, S., Jin, Z., Li, X., Zhu, H., Fang, F., Luo, T., Li, J., 2025. Characterization of microbial carbon metabolism in karst soils from citrus orchards and analysis of its environmental drivers. *Microorganisms* 13 (2), 267.
- Wang, Y., Yin, C., Wang, J., Ji, X., Liu, X., 2024d. The influence of green manure planting on the spectroscopic characteristics of dissolved organic matter in freshwater-leached saline-alkali soil at different depths. *Agronomy* 14 (7), 1546.
- Wang, Y.H., Zhang, P., He, C., Yu, J.C., Shi, Q., Dahlgren, R.A., Spencer, R.G.M., Yang, Z. B., Wang, J.J., 2023b. Molecular signatures of soil-derived dissolved organic matter constrained by mineral weathering. *Fundam. Res.* 3 (3), 377–383.
- Wang, X., Zhou, L., Fu, Y., Jiang, Z., Jia, S., Song, B., Liu, D., Zhou, X., 2024b. Drought-induced changes in rare microbial community promoted contribution of microbial necromass C to SOC in a subtropical forest. *Soil Biol. Biochem.* 189, 109252.
- Wang, W., Zhu, Y., Qu, J., 2024a. Effect of DOM derived from composting on the changes of Pb bioactivity in black soil. *J. Environ. Chem. Eng.* 12, 112232.
- Wu, D., Ren, C., Ren, D., Tian, Y., Li, Y., Wu, C., Li, Q., 2023. New insights into carbon mineralization in tropical paddy soil under land use conversion: Coupled roles of soil microbial community, metabolism, and dissolved organic matter chemodiversity. *Geoderma* 432, 116393.
- Xiao, Y., Huang, R., Xiong, W., Liu, B., Zhou, Q., Jiang, T., Wong, V.N.L., Liu, J., Wu, Y., Luo, Y., Li, Q., Xu, Q., Lan, T., Wang, C., Li, B., 2025. Organic fertilizer intensifies the vertical heterogeneity of DOM in paddy fields through interactions with soil minerals. *Soil Till. Res.* 248, 106454.
- Yan, Y., Wang, C., Zhang, J., Sun, Y., Xu, X., Zhu, N., Cai, Y., Xu, D., Wang, X., Xin, X., Chen, J., 2022. Response of soil microbial biomass C, N, and P and microbial quotient to agriculture and agricultural abandonment in a meadow steppe of northeast China. *Soil Till. Res.* 223, 105475.
- Yang, T., Li, X., Hu, B., Li, F., Wei, D., Wang, Z., Huang, L., Bao, W., 2024a. Climate and soil properties shape latitudinal patterns of soil extracellular enzyme activity and stoichiometry: evidence from Southwest China. *Appl. Soil Ecol.* 197, 105319.
- Yang, X., Zhang, S., Wu, D., Huang, Y., Zhang, L., Liu, K., Wu, H., Guo, S., Zhang, W., 2024c. Recalcitrant components accumulation in dissolved organic matter decreases microbial metabolic quotient of red soil under long-term manuring. *Sci. Total Environ.* 934, 173287.
- Yang, W., Zhu, Y., Jiang, Y., Zhang, J., Wang, W., Jin, Y., Liu, X., Qu, J., 2024b. Dissolve organic matter of mature chicken compost contributes to the protection of microorganisms from the stress of heavy metals. *J. Environ. Chem. Eng.* 12, 113590.
- Yu, B., Liu, D., Bian, Z., Yang, F., 2024. Applying synchronous fluorescence with Gaussian band fitting and MW-2DCOS to assess removals of DOM in acrylic fiber wastewater treatment process. *J. Environ. Chem. Eng.* 12, 112250.
- Zhang, X., Bai, J., Zhang, Z., Xie, T., Zhang, G., Liu, Y., Chen, G., Liu, Z., 2023b. Plant invasion strengthens the linkages between dissolved organic matter composition and the microbial community in coastal wetland soils. *Catena* 232, 107449.
- Zhang, J., Li, Y., Yuan, J., Chi, F., Kuang, E., Zhu, Y., Sun, L., Wei, D., Liu, J., 2024. Analysis of the fluorescence spectral characteristics of dissolved organic matter in a black soil with different straw return amounts. *Sci. Rep.* 14 (1), 29948.
- Zhang, X., Nie, L., Gao, H., Yu, H., Liu, D., 2023c. Applying second derivative synchronous fluorescence spectroscopy combined with Gaussian band fitting to trace variations of DOM fractions along an urban river. *Ecol. Indic.* 146, 109872.
- Zhao, Y., Biswas, A., Liu, M., Han, X., Lu, X., Chen, X., Hao, X., Zou, W., 2025. Land use effects on soil carbon retention through glomalin-mediated aggregation. *Geoderma* 456, 117252.
- Zhao, Z., Geng, P., Wang, X., Li, X., Cai, P., Zhan, X., Han, X., 2023. Improvement of active organic carbon distribution and soil quality with the combination of deep tillage and no-tillage straw returning mode. *Agronomy* 13 (9), 2398.
- Zhou, X., Ma, A., Chen, X., Zhang, Q., Guo, X., Zhuang, G., 2023. Climate warming-driven changes in the molecular composition of soil dissolved organic matter across depth: a case study on the tibetan plateau. *Environ. Sci. Technol.* 57, 16884–16894.
- Zosso, C.U., Ofiti, N.O.E., Torn, M.S., Wiesenberg, G.L.B., Schmidt, M.W.I., 2023. Rapid loss of complex polymers and pyrogenic carbon in subsoils under whole-soil warming. *Nat. Geosci.* 16 (4), 344–348.